INTERNATIONAL JOURNAL OF INTEGRATED ENGINEERING
ISSN: 2229-838X e-ISSN: 2600-7916

IJIE

Vol. 16 No. 4 (2024) 72-81
https://publisher.uthm.edu.my/ojs/index.php/ijie

A Foundational Study on Rational Optimization of Damping Ratio for Accurate Dynamic Simulation with Ultra Large Displacement

Erjon Krasniqi[1]*, Ryuki Nagano[1], Hiroyuki Obiya[1]

[1] *Department of Civil Engineering and Architecture, Saga University, Honjo-machi, Saga, 840-8502, JAPAN*

*Corresponding Author: erjon.kra@gmail.com
DOI: https://doi.org/10.30880/ijie.2024.16.04.010

Article Info

Received: 9 November 2023
Accepted: 29 May 2024
Available online: 15 August 2024

Keywords

Ultra large displacement, tangent stiffness method, Rayleigh damping, FEM

Abstract

The integration of dynamic simulation analysis has become widespread in general-purpose software, providing enhanced capabilities. However, accurately tracking deformations based on complete equilibrium solutions remains a significant challenge in problems characterized by strong geometric nonlinearity. This study examines the accuracy of the combined Newmark β method and Tangent stiffness method in dynamic analysis with ultra large displacements and evaluates the utility of Rayleigh proportional damping in numerical simulations compared to experimental models. An experimental model of a slender steel plate undergoing free vibrations after being released from a deformed state was created. Video footage capturing the deformation histories was compared to computational simulations to verify accuracy. The study also examines the appropriate values of the damping ratio (ζ) and the Newmark β value in the simulations. The results indicate that adjusting various damping ratio and a β value of 1/2 yield more realistic simulations with longer conservation of mechanical energy. The findings suggest that incorporating numerical damping into actual damping settings can achieve a more realistic simulation of dynamic behaviour with ultra-large displacements. Furthermore, experiments and analyses were performed to correct natural frequency by changing Young's modulus, which is a key factor influencing natural frequencies, with observed correlations to plate thickness, setting the stage for further research under varied conditions to develop a more rational methodology for structural analysis.

1. Introduction

Recently, the integration of dynamic simulation analysis has become a standard feature in general-purpose software, providing enhanced capabilities. However, when addressing problems characterized by strong geometric nonlinearity, achieving accurate deformation tracking based on a complete equilibrium solution remains a formidable challenge due to ultra large displacements, material nonlinearity, numerical instabilities, high computational costs, and mesh distortion [1]. Geometrically nonlinear structural analysis heavily relies on the finite element method, which requires the use of various approximation concepts to discretize the nonlinear stiffness equation [2]-[4]. The accurate assessment of the effects of these approximations on the solution through physical considerations remains a complex task. Furthermore, these approximations of FEM introduce cumulative errors during incremental analysis, leading to significant discrepancies in the case of ultra large displacements.

This is an open access article under the CC BY-NC-SA 4.0 license.

Consequently, the elimination of these errors becomes impractical, presenting substantial difficulties in ensuring reliable behaviour tracking.

Considering the above, the combination of the Newmark β method and the Tangent stiffness method [5] offers a favourable approach for achieving accurate solutions in dynamic analysis involving significant displacements. The Newmark β method [6], [7], known for its unconditional stability in linear analysis, it reliably solves dynamic behaviour equations, independent of the chosen time step, making it a preferred choice for various applications in structural engineering and other fields. Meanwhile, the Tangent stiffness method, is a highly advantageous choice for accurately evaluating rigid body displacements in static analysis, particularly when dealing with structures exhibiting large deformations and significant geometric changes. This method excels in capturing the complexities of nonlinear behaviour, which linear theories may not adequately address. By considering higher-order terms in the strain-displacement relationship, the tangent stiffness method provides more realistic and precise results. By leveraging the complementary strengths of these methods, it becomes possible to enhance the reliability and effectiveness of dynamic analyses with ultra-large displacements.

This study aims to assess the accuracy and utility of Rayleigh proportional damping and the aforementioned analysis program through a comparative analysis of experimental models and numerical simulations [8]. The findings will provide insights into rational damping ratio settings and enhance fundamental knowledge in this field.

An experimental model which is to observe free vibration of a slender and thin steel plate after being released from a deformed state of circle shape was created. Using a high speed camera, the video footage capturing the deformation histories, taken after the removal of external forces, was compared to computational simulation to verify its accuracy. The computational simulation was executed by the geometrically nonlinear theory based on the simple displacement method, and solutions fill strictly equilibrium conditions.

Estimation of the damping ratio is complex, influenced by factors such as material micro-level properties, friction, and air resistance in member joints. According to the general way to determine Rayleigh proportional damping coefficients, eigenmode displacement responses under undamped conditions were studied. Natural frequencies of dominant modes were used as initial values for the damping coefficient.

In this study, a discussion for the appropriate value of β is also shown. In general, the mean acceleration method with β =1/4 is used as the most reliable time incremental method, and it is said that 'β =1/4' can realize the conservation of mechanical energy. First, this study examines the appropriate order of damping ratio under the condition of 'β =1/4' by comparison of computational simulation results and a measurement result of the actual behaviour of the model. However, it became evident that using 'β =1/4' makes numerical instability caused by the divergence of mechanical energy so frequently.

Therefore, re-consideration about the time integration method was required, and adopting of 'β =1/2' was suggested for improvement. This causes numerical damping, but longer conservation of mechanical energy could be observed by our examination. It is a breakthrough point of this study to assume that numerical damping can be incorporated into actual damping settings to achieve a more realistic simulation.

As a result, simulation of the model in a long time span could be realized, and it was confirmed that each shape of computational solution during the time range with ultra-large displacement is so reliable match to the corresponding photo captured by video. Furthermore, a series of experiments and numerical analyses were conducted on plates with varying thicknesses to correct natural frequency by changing Young's modulus, which is a dominant factor in natural frequencies. This revealed a correlation between the correction coefficient and plate thickness, setting the stage for future research to accumulate data under diverse conditions and advance a more rational methodology for structural analysis.

2. Tangent Stiffness Method

In structural analysis using the finite element method, the geometric nonlinearity can be separated into two components. The first component is caused by the rigid-body displacement of each finite element, while the second component is caused by the deformation of the element itself. To conduct a geometric nonlinear analysis, both components must be evaluated accurately.

The element deformation can be reduced by using denser finite element partitioning, but the rigid-body displacement cannot be reduced. Therefore, it is crucial to evaluate the first nonlinear component caused by rigid-body displacement precisely, especially in ultra-large deformation regions where nodal displacement increases.

The tangent stiffness method is used to ensure stable and static equilibrium conditions in each element, which only constrain rigid-body displacements. Eq. (1) is the element force equation and shows the stiffness relationship between the element force vector S and the element deformation vector s in the element coordinates with stable support conditions.

$$\mathbf{S} = \mathbf{ks} \tag{1}$$

Int. Journal of Integrated Engineering Vol. 16 No. 4 (2024) p. 72-81

The equilibrium equation gives the relationship between the element force S vector and nodal displacement vector D as shown in Eq. (2).

$$\mathbf{D} = \mathbf{JS} \tag{2}$$

The tangent stiffness equation is formulated using the first-order derivative of the equilibrium equation between the nodal vector in the global coordinate system and the element end force vector in the element coordinate system, provided that the element force equation is complete.

$$\delta\mathbf{D} = (\mathbf{K}_G + \mathbf{K}_0)\delta\mathbf{d} = \mathbf{K}\delta\mathbf{d} \tag{3}$$

where, $\mathbf{K_G}$ is the geometric stiffness matrix, caused by the first nonlinear component due to rigid-body displacement, and $\mathbf{K_0}$ is the element stiffness matrix caused by the second nonlinear component due to the element's deformation described in the element local coordinate

3. Rayleigh damping ratio

In this study, we use Rayleigh proportional damping to compare simulations and actual phenomena in programs for dynamic analysis. The motion equation can be expressed as:

$$\mathbf{M}\ddot{u} + \mathbf{C}\dot{u} + \mathbf{K}u = 0 \tag{4}$$

Assuming that the damping matrix is proportional to the mass matrix and the stiffness matrix, with proportionality coefficients μ and ν, respectively, we obtain the following damping matrix:

$$\mathbf{C} = \mu\mathbf{M} + \nu\mathbf{K} \tag{5}$$

The damping ratio ζ formula is given by:

$$\zeta = \frac{c}{c_0} \tag{6}$$

where c is the actual damping coefficient and c_0 is the critical damping coefficient. And if the same damping ratio ζ_0 is used for all modes, we obtain:

$$\mu = \frac{2\omega_1\omega_2}{\omega_1\omega_2}\zeta_0 \tag{7}$$

$$\nu = \frac{2}{\omega_1 + \omega_2}\zeta_0 \tag{8}$$

Here the natural frequencies ω_1 and ω_2 are chosen based on initial values of main modes' frequencies of the main modes where mode displacement predominates in free vibration analysis without damping.

4. Model

In this study, a cantilever model with ultra-large deformation is used. The model consists of a moment applied on the free edge, which deforms the cantilever into a circular shape to achieve an initial equilibrium state, as illustrated in Fig. 1. The circular shape is obtained through iterative solving and updating with the tangent stiffness equation in a static analysis until the unbalanced force reaches convergence. In this study, the actual behaviour of the model whose conditions are shown in Fig. 1 is observed and examined by comparison with results of computational simulation.

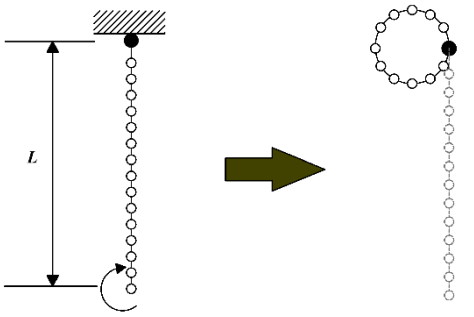

Basic conditions:
L = 1.0 (m)
Cross-section A = 1.75×10^{-5}m^2
Moment of Inertia I = 7.15×10^{-13}m^4
Young's modulus E = 193 GPa
Density ρ = 7930 $\frac{\text{Kg}}{\text{m}^3}$
Material: Stainless steel
(ISO: 4319-301-00-I)

Fig. 1 *A model for numerical example*

The undamped free vibration dynamic analysis is conducted after removing the external force, and the study focuses on the optimization of damping ratio to recreate the actual behaviour. Here, Newmark beta process is adopted. The iteration for geometrical nonlinear analysis to find the displacement to the time step of i+1 from i can be expressed as in Eq. (9) to Eq. (12). If the constant external force can be expressed as:

$$\mathbf{F} = \mathbf{P}(t) + \mathbf{M}\left\{\left(\frac{1}{2\beta}-1\right)\ddot{\mathbf{u}}_i + \frac{4}{\beta\Delta t}\dot{\mathbf{u}}_i\right\} + \mathbf{C}\left\{\left(\frac{1}{4\beta}-1\right)\ddot{\mathbf{u}}_i\Delta t + \left(\frac{1}{4\beta}-1\right)\dot{\mathbf{u}}_i\right\} \tag{9}$$

Here, **P**(t) is external force depending on time, and **M** and **C** are mass matrix and damping matrix respectively. In this paper, we didn't apply damping so **C**=**0**. Further, the unbalanced force of j^{th} iteration can be:

$$\Delta\mathbf{U}_j = \mathbf{F} - \left(\frac{\mathbf{M}}{\beta\Delta t^2} + \frac{\mathbf{C}}{2\beta\Delta t}\right)\Delta\mathbf{u}_{i+1,j} - \mathbf{J}(\Delta\mathbf{u}_{i+1,j})\mathbf{S}(\Delta\mathbf{u}_{i+1,j}) \tag{10}$$

Therefore, we can use the tangent stiffness equation for each iteration step will be:

$$\Delta\mathbf{u}_{i+1,j+1} = \mathbf{K}_{i+1,j}^{-1}\Delta\mathbf{U}_j, \qquad \mathbf{K} = \mathbf{K}_G + \mathbf{K}_0 \tag{11}\ (12)$$

5. Numerical Experiment and Adjusting to Actual Behaviour

5.1 Examination for Appropriate Damping Ratio in Case of β =1/4

In this section, we will discuss how to set the damping constants using the mean acceleration method with β = 1/4, which is a reliable method for small displacement analysis. By this method, we can expect exact solutions with energy conservation under the condition of no-damping for ultra large displacement analyses. Prior to discussing about damping coefficients, free vibration analysis without damping was executed, and the maximum amplitude of displacement is picked up for each mode (Fig. 2). According to this result, the 33$^{\text{rd}}$ mode can be selected as having the most unstable waveform and the highest amplitude. However, as the other mode which should be adopted as one in Eq. (7) and Eq. (8), any other mode except for the 32$^{\text{nd}}$ mode among the 17$^{\text{th}}$ to 32$^{\text{nd}}$ of the secondary higher amplitude group didn't show significant damping. Therefore, the 32$^{\text{nd}}$ and 33$^{\text{rd}}$ are adopted in this study.

Fig. 3 shows a comparison of the time history of horizontal edge displacement depending on the difference of the value of the damping ratio in Table 1.

As a result of this numerical experiment, the findings indicated that the mass proportionality coefficient was significantly more dominant than the stiffness proportionality coefficient. Also, we could find that the order of 1.0×10^{-5} is a match to the experimental data respectively and did not show divergence of mechanical energy. Therefore, we can judge the order to be adequate for the damping ratio of this model. On the other hand, using Newmark β =1/4, that divergence cannot be avoided even in the case of no-damping, and we are forced to adopt quite a small time-increment of 1.0×10^{-4} s. Fig. 4 shows the chaotic shape of the solution when the energy divergence occurred in case that $\zeta = 1.0\times10^{-2}$ was adopted. Consequently, it is unstable to use Newmark β = 1/4 for ultra-large deformational analysis just like in this case, and we have to modify the time incremental method.

Int. Journal of Integrated Engineering Vol. 16 No. 4 (2024) p. 72-81

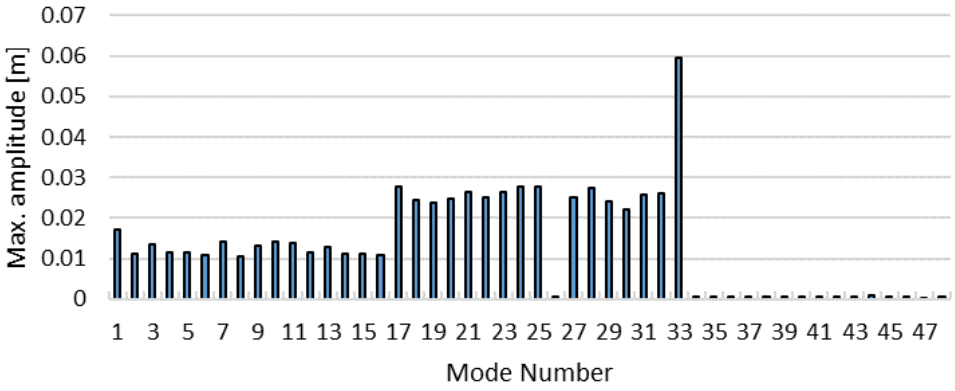

Fig. 2 *Maximum amplitude of displacement for each mode*

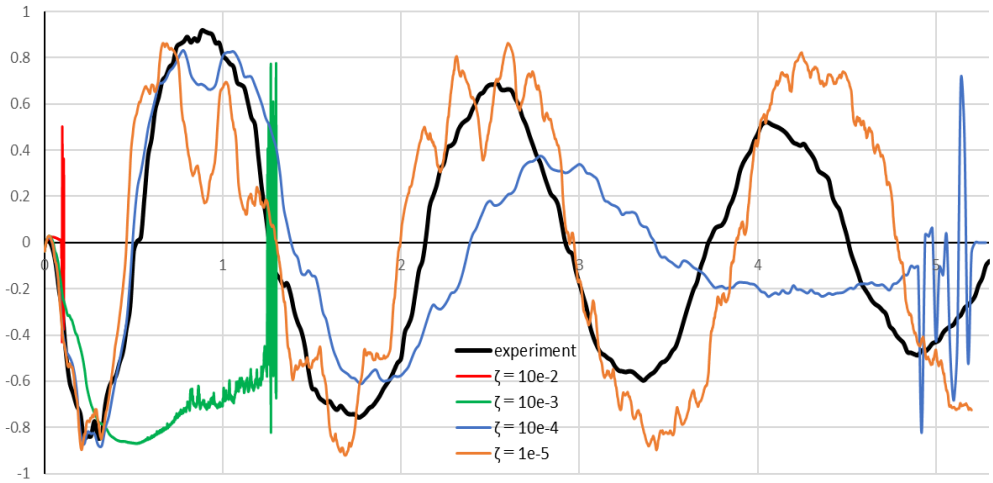

Fig. 3 *Time history of horizontal edge displacement*

Fig. 4 *Shape of solution in divergence case*

Table 1 *Examined damping ratio and coefficients*

Damping ratio, ζ	μ	ν	Time to energy divergence, s
1.0×10^{-2}	1.38×10^{2}	7.17×10^{-7}	0.09
1.0×10^{-3}	1.38×10^{1}	7.17×10^{-8}	1.2
1.0×10^{-4}	1.38×10^{0}	7.17×10^{-9}	4.9
1.0×10^{-5}	1.38×10^{-1}	7.17×10^{-10}	After 30

5.2 Re-consideration of Newmark β value

In this section, the relation between the Newmark β value and energy conservation in the case of free vibration analysis without damping is investigated, and it is discussed about suitable β value [9]. The study tested 25 different β values, ranging from 0.2 to 0.5 at intervals of 0.0125, and the duration of energy conservation is examined for each β value. The termination point of duration is defined when the energy exceeds five time of the initial energy. The results indicated that a higher β value tends to realize a longer duration, as illustrated in Fig. 5.

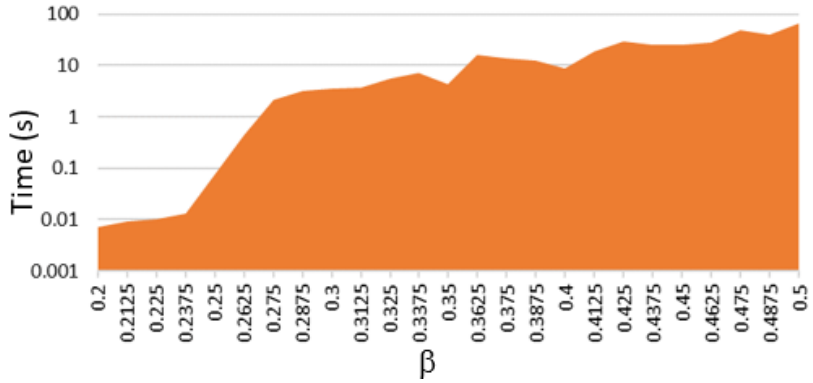

Fig. 5 *Relation between conservation duration and β*

Fig. 6 shows as energy time history with β=1/2 under non-damping conditions. Here, the numerical damping of gradual energy decreasing can be observed. Despite this, using β=1/2 can still suppress energy divergence and amplification. Hence, it is suggested that numerical damping can be incorporated into actual damping settings to achieve a more realistic simulation.

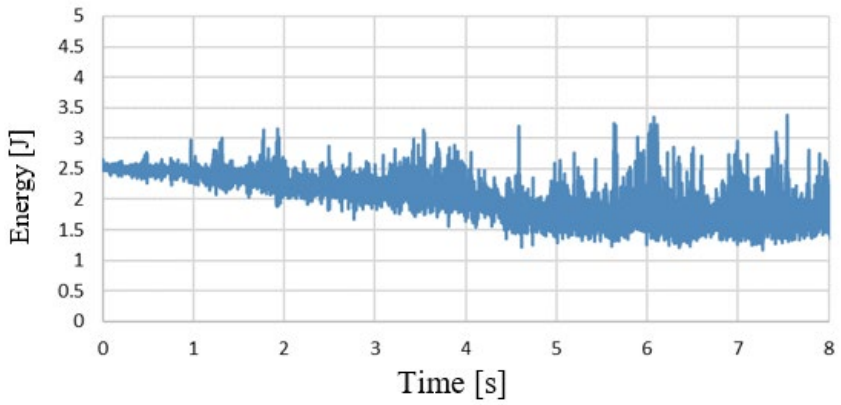

Fig. 6 *Numerical damping of energy when β=1/2*

Fig. 7 shows a comparison of horizontal displacement response between the simulations with $\zeta = 1.0\times10^{-5}$, $\zeta = 3.0\times10^{-5}$ for each by β=1/2 $\Delta t = 1.0\times10^{-2}$, and actual behaviour by experiment. In the case of $\zeta = 1.0\times10^{-5}$, the analysis is executed quite stable even under the condition of so large time increment of 1.0×10^{-2}(s) which is 100 times of upper limit when β=1/4 is adopted. However, when $\zeta = 3.0\times10^{-5}$ is substituted to be adjusted to real phenomenon, divergence of mechanical energy has occurred around t =6s. Fig. 8 is the shape of solution just before appearance of divergence, and we can observe that higher mode becomes dominant even in the process toward damping convergence. Therefore, how to suppress the higher mode in damping process may become problem to be solved.

Int. Journal of Integrated Engineering Vol. 16 No. 4 (2024) p. 72-81

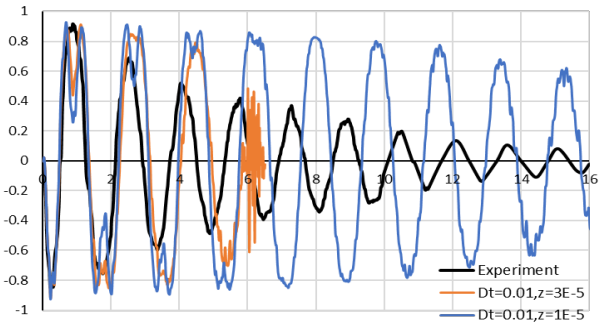

Fig. 7 *Time history of horizontal displacement with* $\beta = 1/2$, $\Delta t = 1.0\times10^{-2}s$

Fig. 8 *Shape of solution just before divergence* ($\zeta = 3.0\times10^{-5}$)

Fig. 9 compares the shape of the numerical solution of the simulation with the behaviour of the experimental model and shows that the displacements of all nodes are generally well reproduced in the phase immediately after the start of vibration, which involves very large displacements.

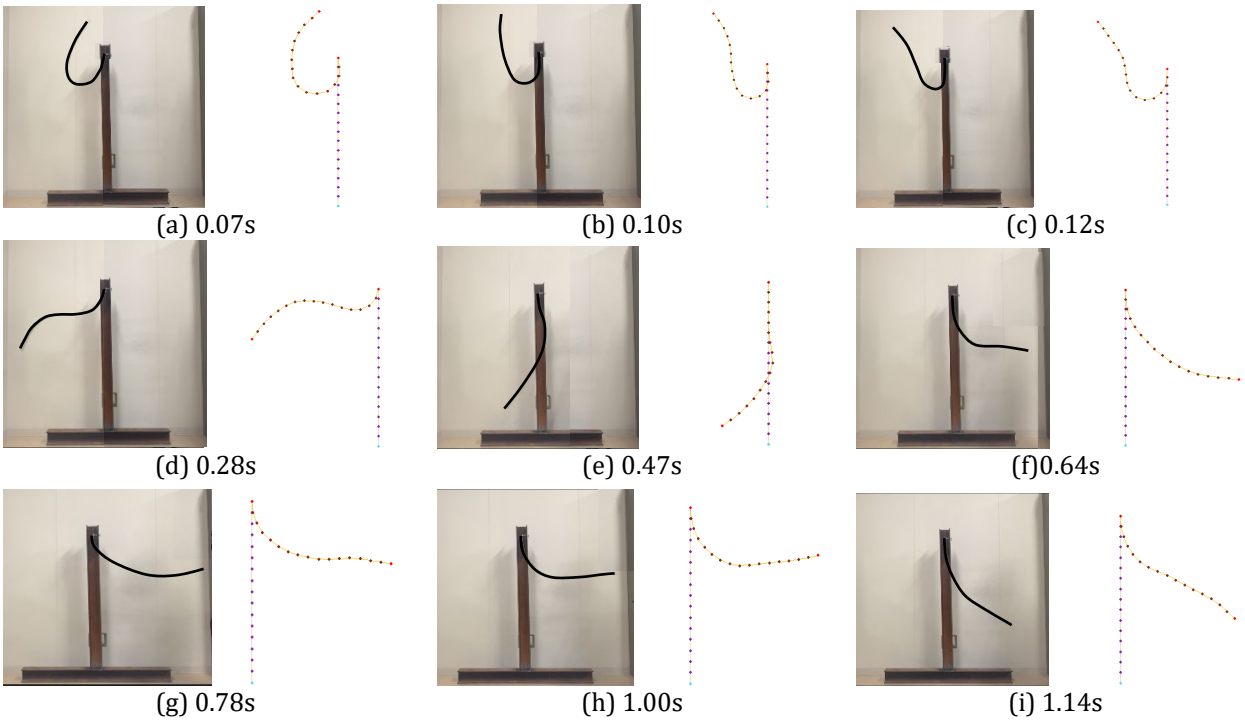

Fig. 9 *Actual behaviour (left side) and simulation (right side)*

5.3 Adjustment of Damping Ratio and Phase Shift to The Result of The Actual Behaviour of The Model

By consideration in the previous section, the possibility that a rougher time increment can be adopted by 'β=1/2' was suggested. Here, we shall discuss how to adjust it to actual behaviour in this section. For the time increment, $\Delta t = 1.0\times10^{-3}$ is used, it is more reasonable than in the case of 'β=1/4' and more stable than in the case of 'β=1/2' and $\Delta t = 1.0\times10^{-2}$. Moreover, by the result until the previous section, adoption of $\zeta = 3.0\times10^{-5}$ can be expected more strict adjustment between real and simulation.

In Fig. 10, the time history of horizontal displacement is depicted, comparing it with the actual structural behaviour. The data from the experiment is represented by the black curve, while the data from the initial simulation is shown by the orange curve. Importantly, a phase difference is observed between these two sets of data, necessitating a correction of the natural frequency. To affect this correction, a modification of the Young's modulus in the simulation was made. The Young's modulus was adjusted from the actual value of E = 193 GPa to E = 330 GPa, as indicated by the blue curve in the figure, this adjustment enabled a more precise alignment of the simulation with the experimental results, minimizing the phase shift in the data.

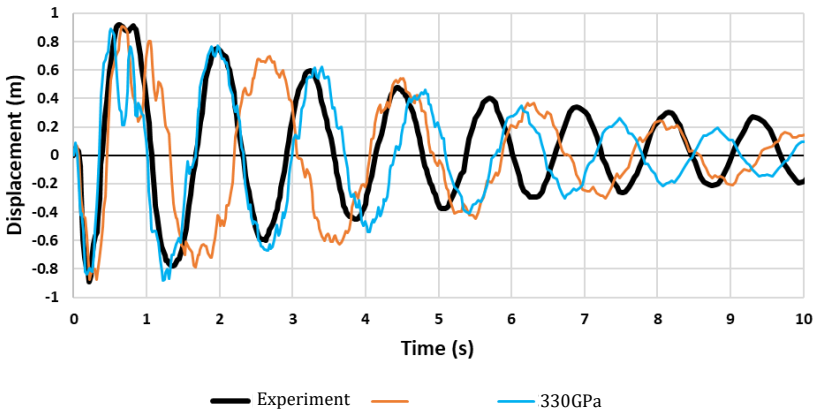

Fig. 10 *Time history of horizontal displacement (plate thickness 0.7 mm) β =1/2, Δt* = 1.0×10^{-3}*s, ζ* =3.0×10^{-5}

Up until here, the simulations and experiments were conducted with a plate thickness of 0.7 mm. Fig. 11 compares the time-history response of horizontal displacement when the plate thickness is changed to 0.8 mm. It compares the measured values with the calculated results based on the actual Young's modulus of 193 GPa and the calculated results with a Young's modulus corrected to 310 GPa.

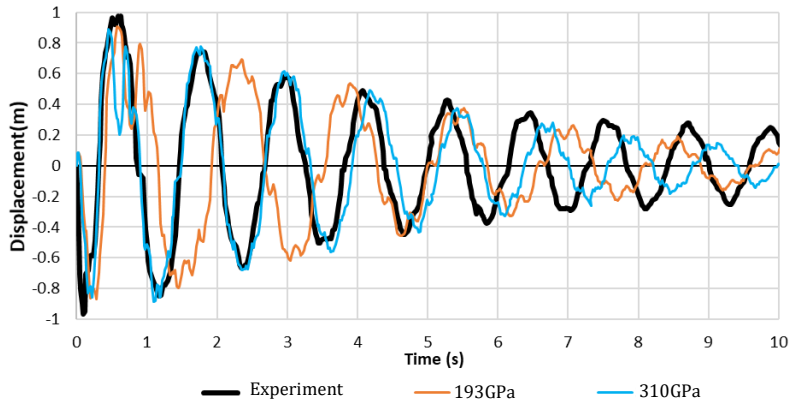

Fig. 11 *Time history of horizontal displacement (plate thickness 0.8mm), β = 1/2, Δt*= 1.0×10^{-3}*s, ζ* = 4.25×10^{-5}

The primary natural frequency of the cantilever beam's bending vibration is expressed as:

$$\omega_{i=1} = \left(\frac{1.8751}{L}\right)^2 \sqrt{\frac{EI}{\rho A}} \tag{13}$$

Therefore, in this case, a correction factor of $\sqrt{(310/193)} = 1.27$ is applied to the natural frequency. It's important to note that a damping ratio $\zeta = 4.25\times10^{-5}$ is used in this analysis.

To investigate a reasonable correction coefficient method for this phase difference, experiments were conducted with six different samples by varying the plate thickness of the model to 0.5 mm, 0.6 mm, 0.7 mm, 0.8 mm, 0.9 mm, and 1.0 mm. Similar to the previous case, the behaviour in experiments and numerical calculations was compared, and the Young's modulus influencing the natural frequency was corrected. Based on this, the study examined correction coefficients that exhibit good reproducibility over several cycles, as seen in Fig. 11.

Int. Journal of Integrated Engineering Vol. 16 No. 4 (2024) p. 72-81

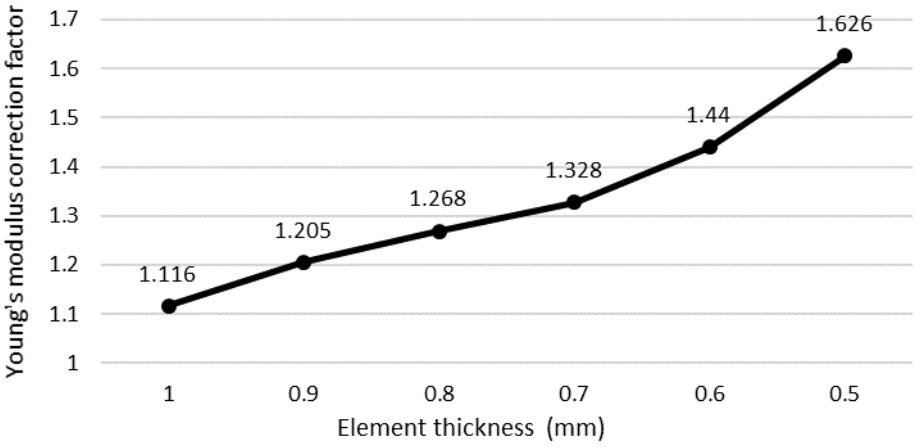

Fig. 12 *Correction factor for each element*

6. Conclusion

This study aimed to evaluate the effectiveness and reproducibility of a dynamic large deformation analysis program using the tangent stiffness method to simulate the deformation history of an experimental model. For the evaluation of the damping phenomenon, it was crucial to set an appropriate damping ratio to achieve consistency in the simulation, rather than relying on the natural frequency of the mode.

The Newmark β method with a value of β set to $1/2$ was found to suppress energy divergence and replicate real behaviour. Integrating numerical damping into actual damping could lead to reasonable simulations.

At the same time, some new challenges have become evident when 'β =1/2' is adopted. One challenge of damped 'β =1/2' analysis is that computational instability has been detected when the process closes to stationary under the condition of rough time increment in which undamped free vibration produces a stable response. It can be considered that the higher modes of displacement become dominant even in small displacement situations.

The second challenge originated from the fact that the simulation predicted lower natural frequencies compared to the actual values, and it revealed phase discrepancies between experimental data and simulation results. In this study, numerous experiments and numerical analyses were conducted on models with different plate thicknesses, with an attempt made to correct the natural frequency by changing Young's modulus, which dominantly influences the natural frequencies. It was observed that the correction coefficient correlated with plate thickness. In the future, further research will involve the accumulation of data under various conditions, including the use of different material lengths and different initial states of damping-free vibration, contributing to the development of a more rational methodology.

Overall, this study provides fundamental knowledge for the evaluation of a dynamic large deformation analysis program and addressing damping phenomenon, offering valuable insights for enhancing accuracy in simulating complex nonlinear behaviour.

Acknowledgement

A part of this work was supported by JSPS KAKENHI Grant Number JP 23K04007.

Conflict of Interest

Authors declare that there is no conflict of interests regarding the publication of the paper.

Author Contribution

The authors confirm contribution to the paper as follows: ***study conception and design:*** *Erjon Krasniqi and Hiroyuki Obiya,* ***data collection:*** *Erjon Krasniqi and Ryuki Nagano;* ***analysis and interpretation of results:*** *Erjon Krasniqi, Ryuki Nagano and Hiroyuki Obiya,* ***draft manuscript preparation*** *Erjon Krasniqi, Ryuki Nagano and Hiroyuki Obiya. All authors reviewed the results and approved the final version of the manuscript.*

References

[1] Nguyen, T. L., Sansour, C., & Hjiaj, M. (2017). Long-term stable time integration scheme for dynamic analysis of planar geometrically exact Timoshenko beams. Journal of Sound and Vibration, 396, 144-171. https://doi.org/10.1016/j.jsv.2017.03.024

[2] Simo, J. C., & Tarnow, N. (1992). The discrete energy-momentum method. Conserving algorithms for nonlinear elastodynamics. Zeitschrift für angewandte Mathematik und Physik ZAMP, 43, 757-792. https://doi.org/10.1007/BF00913408
[3] Chhang, S., Sansour, C., Hjiaj, M., & Battini, J. M. (2017). An energy-momentum co-rotational formulation for nonlinear dynamics of planar beams. Computers and Structures, 187, 50-63. https://doi.org/10.1016/j.compstruc.2017.04.003
[4] Chung, J., & Hulbert, G. M. (1993). A time integration algorithm for structural dynamics with improved numerical dissipations: the generalized-alpha method. Journal of Applied Mechanics, 60, 371-375. https://doi.org/10.1115/1.2900803
[5] Nizam, Z. M., Obiya, H., Ijima, K., & Azhar, A. T. S. (2015). A comparison for the simulation of frictionless contact problem with large displacement. Applied Mechanics and Materials, 773-774, 257-261. https://doi.org/10.4028/www.scientific.net/AMM.773-774.257
[6] Newmark, N. M. (1959). A method of computation for structural dynamics. Proceedings of the American Society of Civil Engineers, 85, 64-94. https://doi.org/10.1061/JMCEA3.0000098
[7] Belytschko, T., Liu, W., & Moran, B. (2000). Nonlinear Finite Elements for Continua and Structures. John Wiley & Sons, pp. 329-357.
[8] Wang, H. F., & Zhang, R. L. (2019). A method for determining Rayleigh damping parameters of complex field. Civil Engineering Journal, 28, 420-434.
[9] Krasniqi, E., Yamashita, S., & Obiya, H. (2022). Study on energy conservation in dynamic ultra-large deformation analysis of plane frame structures. In Proceedings of the International Conference on Computational Methods, https://www.sci-en-tech.com/ICCM2022/ICCM2022-Proceedings.pdf
[10] Belytschko, T., & Hughes, T. (1983). Computational Methods for Transient Analysis. North-Holland Pub.